Marine Geodesy, 27: 433–451, 2004

ISSN: 0149-0419 print / 1521-060X online
DOI: 10.1080/01490410490902007

Taylor & Francis
Taylor & Francis Group

Altimeter Signal-to-Noise for Deep Ocean Processes in Operational Systems

KIRK R. WHITMER
GREGG A. JACOBS

Naval Research Laboratory
Stennis Space Center
Mississippi, USA

OLE MARTIN SMEDSTAD

Planning Systems Incorporated
Stennis Space Center
Mississippi, USA

The ocean signal for this study is the sea surface height due to the slowly varying (greater than 5-day) ocean processes, which are predominantly the deep ocean mesoscale. These processes are the focus of present assimilation systems for monitoring and predicting ocean circulation due to ocean fronts and eddies and the associated environmental changes that impact real time activities in areas with depths greater than about 200 m. By this definition, signal-to-noise may be estimated directly from altimeter data sets through a crossover point analysis. The RMS variability in crossover differences is due to instrument noise, errors in environmental corrections to the satellite observation, and short time period oceanic variations. The signal-to-noise ratio indicates that shallow areas are typically not well observed due to the high frequency fluctuations. Many deep ocean areas also contain significant high frequency variability such as the subpolar latitudes, which have large atmospheric pressure systems moving through, and these in turn generate large errors in the inverse barometer correction. Understanding the spatial variations of signal to noise is a necessary prerequisite for correct assimilation of the data into operational systems.

Keywords satellite altimetry, Jason-1, TOPEX/Poseidon, ERS, GFO, near real time, sea surface height, mesoscale features, data assimilation

Altimeter observations provide a direct measure of the ocean dynamic state. The sea surface height (SSH) provides the barotropic pressure gradient. Throughout much of the deep ocean, the internal ocean variability is not barotropic but rather baroclinic. Within these areas, the baroclinic variability has a few vertical modes and has strong correlations to the SSH (Hallock et al. 1989). The SSH can thus be used to infer the internal ocean environment, and this property has proved to be very important to SSH assimilation into ocean numerical models (Blayo et al. 1994, 1997; Fox et al. 2000; Segschneider 1999).

Received 24 May 2004; accepted 7 October 2004.

Two reviewers provided valuable comments that significantly improved this manuscript. This work was sponsored by the SPAWAR project "Altimeter Data Fusion Center Support" and the NRL project "Slope to Shelf Energetics and Exchange Dynamics." This article is NRL paper contribution number NRL/JA/7320/04/0009.

Address correspondence to Kirk R. Whitmer, NRL 7320, Stennis Space Center, MS 39529. E-mail: whitmer@nrlssc.navy.mil

Ocean assimilation models and satellite observations must be viewed as pieces of the same system, and the requirements and capabilities must match. The ocean assimilation model must accurately represent, and the satellites must sufficiently observe the ocean processes. The ocean assimilation model must take into account the observation accuracy to combine properly the satellite observations with the numerical dynamics that represent the true ocean (Robinson et al. 1998). In addition to knowledge of the observation accuracy, it is important to understand the relative magnitude of observation errors to the signal of interest. This provides an indication of in which areas it would be expected that the ocean system would provide accurate results.

When the ocean assimilation model and observation systems are designed, the central focus is the ocean process. For altimeter observations and for global systems that provide the deep ocean environment, the dominant processes are first mode baroclinic features that generate nondeterministic fronts and eddies. The effects are of large importance to the fishing industry, off-shore oil drilling operations, search and rescue, and ship routing (Chen et al. 2004). Eddy features typically have long time periods up to scales of years (Schouten et al. 2000), and this feature can be used as a simple method to separate the signal, which will be the deep ocean mesoscale within this study, from the noise, which for purposes here will be all other higher frequency processes.

One method to estimate the noise level is by crossover analysis, and this has been standard practice within the altimetry community. The points at which the satellite ground track crosses itself provide an excellent location to observe sea level variability on time periods longer than half the satellite repeat period (five days for Jason-1). At the crossover points, the contribution to the SSH from the steady-state ocean circulation and the geoid are constant in time and the same for ascending and descending passes. Thus, differencing SSH at the crossover points cancels any errors in geoid or ocean mean dynamic height. By constructing a mean sea level based on the observations themselves, the mean orbit solution error is removed and is not an influence. At time periods much greater than the time separation, crossover differences due to ocean SSH changes observed by the ascending and descending passes should be roughly equal, and thus differencing SSH should remove what is taken to be the signal in this study. The remainder of the difference is then noise. Of course, we must keep in mind that a portion of the total fluctuations in the mesoscale field occur at time periods less than five days. An examination of the noise calculated at the crossover points indicates that the induced error is largest in the high northerly latitudes, shelf regions, and in areas of the Gulf Stream and Kuroshio.

Obviously, the highest possible level of accuracy is desired, and error budgets for the altimeters such as Topex/Poseidon and Jason-1 are approaching the 3cm level (Zanifé et al. 2003). These values are based on a global average, however, and do not provide insight as to the error for specific regions. So questions that often arises are how does the altimeter data accuracy vary throughout the globe, and is this accuracy sufficient to observe the local mesoscale variability? In areas of large amplitude eddies and current meanders such as the Gulf Stream, Kuroshio, and Aghulas currents, the signal is large enough that typical errors in altimeter measurement systems are much smaller than the signal. In areas such as the Japan/East Sea or eastern subtropical gyres, variations due to eddies are quite small. Thus, improved knowledge of the errors and error level relative to the signal for each geographic region is highly desirable. By understanding the areas of poor signal to noise and understanding the contributors to noise for the area, improvements can be targeted to achieve the greatest effect. Of even greater interest, especially in the field of ocean modeling, is a quantification of a signal to noise ratio for proper assimilation of the data.

For this study, a method is developed to examine the ratio of signal to noise variance at altimeter track crossover points. These calculations are done for each of the five recent satellite altimeters: Topex/Poseidon, Jason-1, ERS-1, ERS-2, and GFO. The altimeter data

to this data set as well. The calculation of these additional tidal corrections is performed in a separate processing run. This final tidal correction to T/P and Jason-1 provides the largest gain in shallow water regimes where the global tide models are known to have the largest errors.

An orbit correction is calculated and applied to the height data. This correction is calculated through fitting a once-per-revolution sinusoid to each track, where a track is defined as the satellite traversing from the pole to that same pole. Before doing this fit the mean sea surface height must be removed. In addition, the seasonal steric anomaly must be taken into account, as this signal would easily be aliased into a sinusoidal fit. Because the steric anomaly cannot be independently measured or perfectly modeled, it is approximated with climatological values from GDEM (Teague et al. 1990). The mean sea surface height computation for each satellite is explained in more detail below. The mean height plus the seasonal steric anomaly provide the seasonal mean height. The once-per-revolution sinusoid is fit to the the SSHA minus the seasonal mean height . An iterative approach is used so as to identify outliers which can then be removed from the calculation of the fit. At the end of this calculation the orbit correction is applied to the data and the long term mean removed from the data. This yields the SSHA.

The mean sea surface height is calculated at each reference track point for each satellite altimeter mission. This calculation was first completed for the 10 years of the T/P mission. Because of the precision and accuracy of this mission, knowledge from it is used to assist in the calculations of the GFO and ERS-1/2 mean sea surface heights. A mesoscale interpolation of the T/P data is first constructed. The mesoscale interpolation constructs a weighted average of the SSHA data at each point in space and time. The weighting is a Gaussian function of the form:

$$W(x, y, t) = \mathrm{Exp}\left(-\left[\frac{(x-ut)^2}{L_x^2} + \frac{(y-vt)^2}{L_y^2} + \frac{t^2}{T^2}\right]\right). \tag{1}$$

The coefficients of the longitudinal length scale L_x^2, the latitudinal length scale L_y^2, the propagation speed in the zonal direction u, the propagation speed in the meridional direction v, and the time decorrelation T are taken from Jacobs et al. (2001).

The result is then interpolated in space and time to the GFO or ERS-1/2 ground tracks and subtracted from the altimeter SSH. The purpose of this is so that the altimeter SSHA observations would be anomalies from a mean over a common time period (the first 10 years of the Topex/Poseidon mission). Note that the T/P mean surface height is also used for Jason-1. Thus, the SSHA from all data sets is consistently a SSHA from the same time period.

For this study a smoothing is performed on each of the respective SSHA data sets. A 3-second e-folding length Gaussian filter is applied along track. This lowers the white noise associated with the measurements.

Assuming that the SSHA and noise are uncorrelated, the signal to noise ratio is computed for each altimeter data set at crossover points for each altimeter using the following equation:

$$\frac{\mathrm{var}\langle \mathrm{ssh}\rangle}{\mathrm{var}\langle \varepsilon\rangle} = \frac{\mathrm{var}\langle \mathrm{ssh}+\varepsilon\rangle - \mathrm{var}\langle \varepsilon\rangle}{\mathrm{var}\langle \varepsilon\rangle}. \tag{2}$$

The variance of the noise (var $\langle\varepsilon\rangle$) at each crossover point is computed by:

$$\mathrm{var}\langle \varepsilon\rangle = \frac{\sum_{i=1}^{N} [(\mathrm{SSHA}_i - \mathrm{SSHA}_j) - \overline{\mathrm{SSHA}}]^2}{N-1}. \tag{3}$$

is first processed to produce sea surface height anomalies (SSHA), and the corresponding signal-to-noise ratio is computed. The results are examined in detail. Finally, the results are interpreted in terms of causes of low signal-to-noise and proposed methods for improvement. Some explanation is given as to why, in regions where the signal-to-noise ratio is less than one, the altimeter may still be returning valuable oceanographic information. To achieve this, a particular feature must be observed by more than one sample. Combining observations through optimal interpolation or dynamical model assimilation can achieve this.

Methodology

All satellite altimeter data available up to June 2003 are included in the analysis: Jason-1, GFO, TOPEX/Poseidon (T/P), ERS-1, and ERS-2. The data from the ERS-1, and ERS-2 missions are combined and evaluated as one set (ERS-1/2). When overlap in time occurs, the data from ERS-2 is preferentially used. Each of these data sets is processed separately, but in a very similar manner. The only differences in processing occur in checking flags on the geophysical data records (GDRs) and the source of particular corrections supplied on the GDRs. Note that, for the purposes of this article, the term GDR is used generically to indicate any source files of altimeter data. As this procedure is explained, special note is made of differences in the processing of each altimeter data set. It is also important to note that at each step of the processing quality checks flag suspect data and remove the data from further consideration. These techniques are explained.

Initially the data are read in from the GDRs. The Jason-1 data used are the IGDR files produced by the Jet Propulsion Laboratory (JPL) with orbit solutions based on both DORIS and laser ranging. The GFO data are from GDRs produced by the U.S. Naval Oceanographic Office using orbit solutions based on laser ranging. The T/P data are from the merged GDRs (MGDR) produced by JPL with orbit solutions based on laser ranging and DORIS. The ERS-1/2 data are from GDRs produced by NOAA with laser ranging orbit solutions. All standard environmental corrections (wet and dry troposphere, ionosphere, electromagnetic bias, and inverse barometer corrections) are applied from the GDRS. Each of these corrections is examined along track relative to neighboring values to check for values outside expected limits. If a bad geophysical correction or AGC value is found, the datum is flagged as an outlier. The AGC values are examined by first computing their mean and standard deviation along each track. Any AGC value that is then found to be greater than 3.5 standard deviations from the mean is considered an outlier. Tidal corrections are not applied from the GDR. For internal consistency a single tide model was selected to be used for all data sets. This is explained in more detail below.

The height data is interpolated to reference ground tracks. This interpolation is improved through the use of a map of cross-track geoid gradients. This method uses values from the map described in Sandwell and Smith (1997). It has been demonstrated that this method greatly improves the accuracy of the interpolation, especially in cases such as the later stages of ERS-2 when the satellite deviates by more than 1km from the reference ground track. As a final check for outlier data, SSH values more than four standard deviations from a smoothed SSH are flagged as suspect. The smoothed SSH is calculated along track using a Gaussian filter with e-folding scale of 20 km.

Ocean tide corrections are now applied. The most recent version of the Global Ocean Tide Model, got 00.2, (Schrama and Ray 1994) is applied to all data. This ensures uniformity throughout all data types. In the case of T/P and Jason-1, a further tidal correction is applied. This correction is calculated through the fitting of the eight major ocean tide frequencies to the full 10 years of the T/P SSHA data. The high precision of the T/P mission permits the calculation of this correction. The coincident orbit of the Jason-1 satellite allows application

The above equation is utilized where j represents the nearest cross track point in time to the observation at time i. Assuming the relatively slow change in sea state, the computed variance at each crossover point represents the altimeter noise (including instrument noise, errors in environmental corrections to the instrument, and short time period SSH variability). Since the implied assumption of a steady state ocean breaks down with greater passage of time, crossover points that have the greatest time difference will have larger amounts of actual sea surface signal contained in them. Figure 1 presents the time difference associated with each crossover point based on latitude, because the time difference is dependent on latitude. For a given latitude, the crossover time between ascending and descending passes is constant. Because the T/P and Jason-1 missions have exact repeat times of just less than 10 days the time between crossovers is less than five days, and these data are expected to have the best estimates of noise. That is, the noise estimate is not contaminated by mesoscale related variability.

The total SSHA variance at each crossover point ($\mathrm{var}\langle \mathrm{ssh} + \varepsilon \rangle$) is then computed by:

$$\mathrm{var}\langle \mathrm{ssh} + \varepsilon \rangle = \frac{\sum_{i=1}^{N} (\mathrm{SSHA}_i - \overline{\mathrm{SSHA}})^2}{N - 1}. \tag{4}$$

These values contain the sum of altimeter measured signal plus noise. This variance is computed over all time for each data set up to many years. The signal-to-noise ratio is then able to be computed for each crossover point.

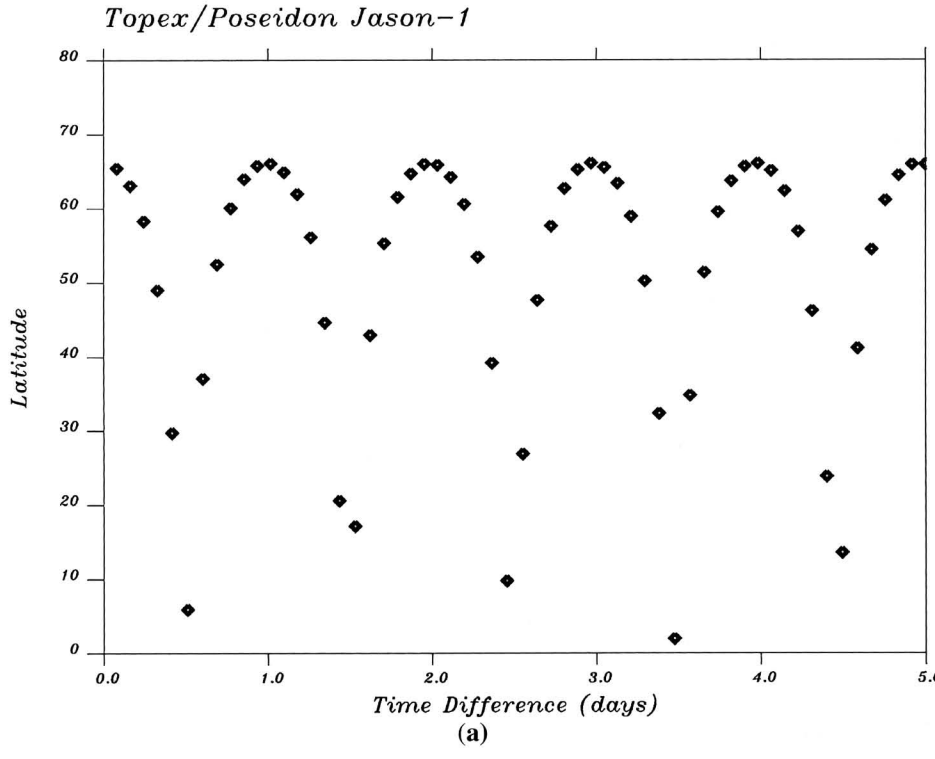

FIGURE 1 The time difference at crossover points is plotted as a function of latitude for each of the three satellite altimeter orbit configurations. Note that the scale of the Time Difference axis varies with length of the respective orbit. The vertical dotted line on the lower two plots represents the maximum time difference associated with the Topex/Poseidon and Jason-1 missions. *(Continued)*

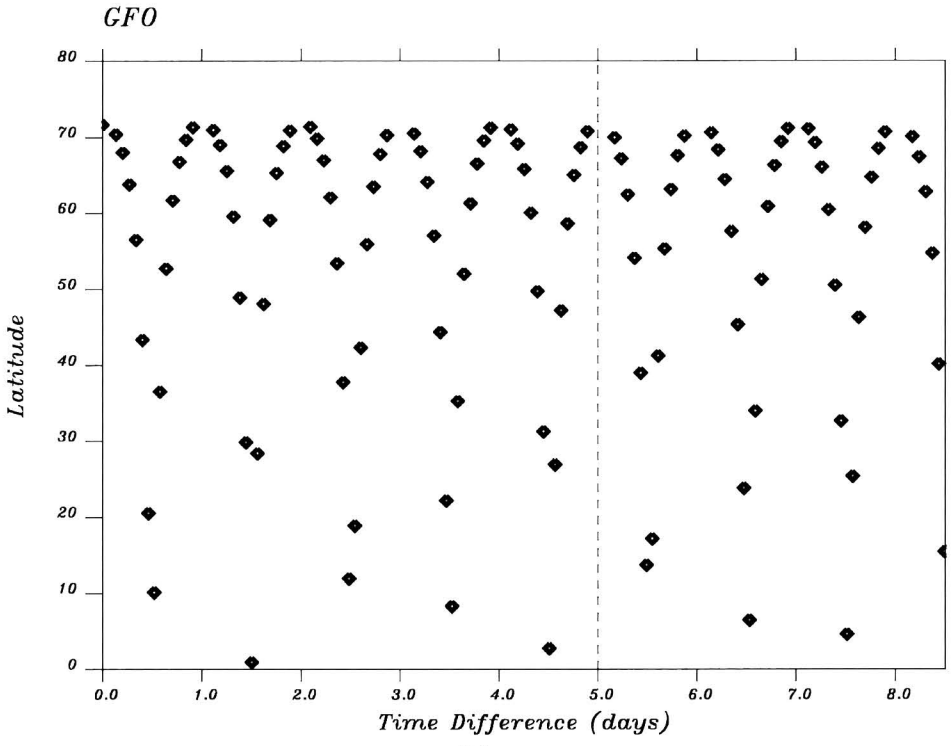

(b)

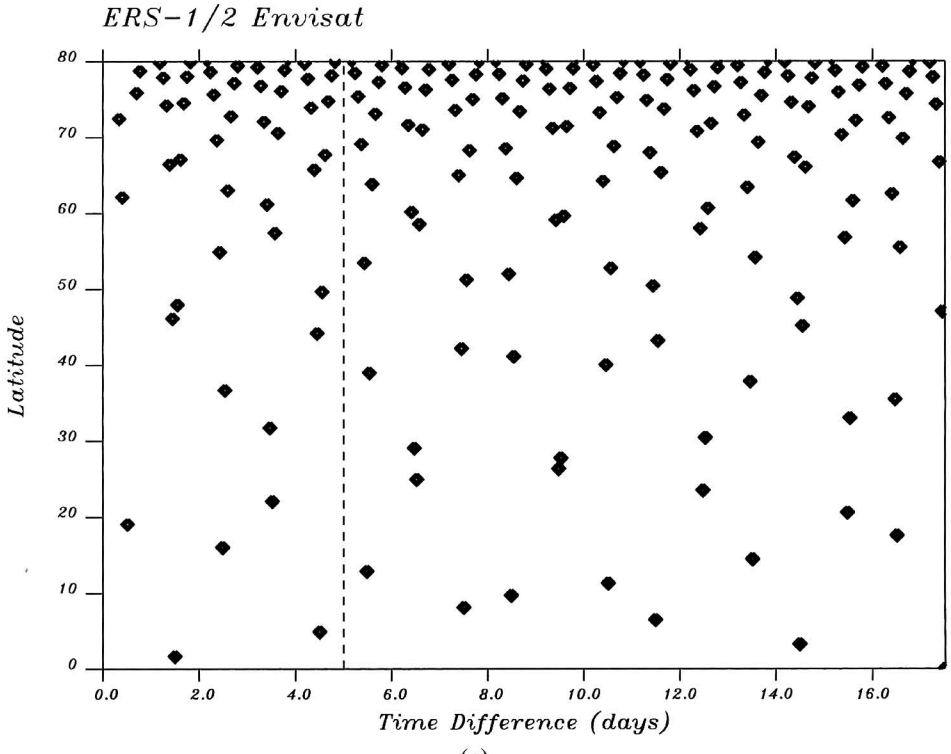

(c)

FIGURE 1 (Continued)

Results

To understand better the global structure of the noise associated with each altimeter, $\mathrm{var}\langle\varepsilon\rangle$ is presented in Figure 2. As expected, the highest values occur at high northerly latitudes, near land and along shelf regions, and in the areas of strong baroclinic currents such as the Antarctic Circumpolar Current, Kuroshio, and Gulf Stream. Coastal regions experience more data outage and higher errors as time is required for the altimeter to regain or maintain track as it leaves or enters the area over the land mass. In addition, larger errors on the shelf are expected. Coastal areas are associated with high frequency variability due to tides (or errors in tide solutions for the SSHA used here) and wind-forced setup and setdown that are aliased into the error variance calculation. Some short time period variability in the major western boundary currents and Antarctic Circumpolar Current also appear as noise. The high northerly latitude regions exhibiting large noise values are coincident with shallower or shelf regions, thus explaining why this behavior is not seen in the southerly latitudes. Overall, the regional structure is seen to be similar for all altimeter missions. ERS-1/2 shows the highest overall noise level and also has higher values in the most southerly latitudes. Some of this can be explained by the fact that ERS-1/2 has a more nearly polar orbit and thus measures at higher latitudes than those sampled by T/P and Jason-1. These regions are highly affected by sea ice. In regions with seasonal sea ice, a much shorter sea height data set is created and thus a less well-defined error accuracy. Sea ice values are not always easily detected and sometimes do not get flagged. Sea ice produces spuriously high SSHA RMS.

Jason-1 and T/P have a significantly higher signal-to-noise ratio than that of GFO and ERS-1/2 (Figure 3). T/P and Jason-1 exhibit very similar values, but Jason-1 outperforms T/P on a global basis, demonstrating a globally averaged signal-to-noise ratio of 0.79 compared to 0.64 for T/P. Jason-1 and T/P both demonstrate globally averaged signal-to-noise ratios two and a half times better than GFO, and ERS-1/2 actually has a negative global mean. This final negative value is not physically realistic. By definition, a variance has a nonnegative value and the ratio of two variances would also have a nonnegative value. It is, however, an artifact of the method used in computing the altimeter signal to noise for this article. Anytime the variance of the crossover differences at a point is greater than the corresponding height variance the resulting ratio is negative. The longer repeat times associated with GFO and ERS-1/2 and the subsequent greater time differences at crossover points increase the likelihood of a large crossover difference height variance. To facilitate a more balanced comparison, further analyses are constructed that included only crossover time differences of less than five days, the maximum associated with the Jason-1 and T/P missions. This significantly improves the mean of GFO to 0.43. ERS-1/2 is also improved, but only to a mean of 0.12. Both of the new plots exhibit distinct bands of no data because of the dependence of time difference on latitude.

As mentioned above, Jason-1 and T/P exhibit comparable means, but the Jason-1 signal to noise values contain more scatter than those of T/P. This is seen most clearly by examining the values in the Antarctic Circumpolar Current and the higher latitudes of the North Pacific where the T/P ratios are much more spatially uniform. This behavior is further supported by the standard deviations of signal to noise of 1.85 for T/P and 2.14 for Jason-1. One possible factor contributing to this is the much longer time series provided by the T/P altimeter providing a more accurate estimate of the noise. To further investigate this, a subset of T/P data was examined. The data selected are from a similar time period of the Jason-1 and the same length as the Jason-1 data set. The resultant statistics are very similar to that already found for Jason-1; a mean of 0.72 compared to Jason-1's 0.79 and a standard deviation of 2.13 compared to Jason-1's 2.14. Thus much of the scatter associated with Jason-1 can be explained through the short mission life at the time of this article.

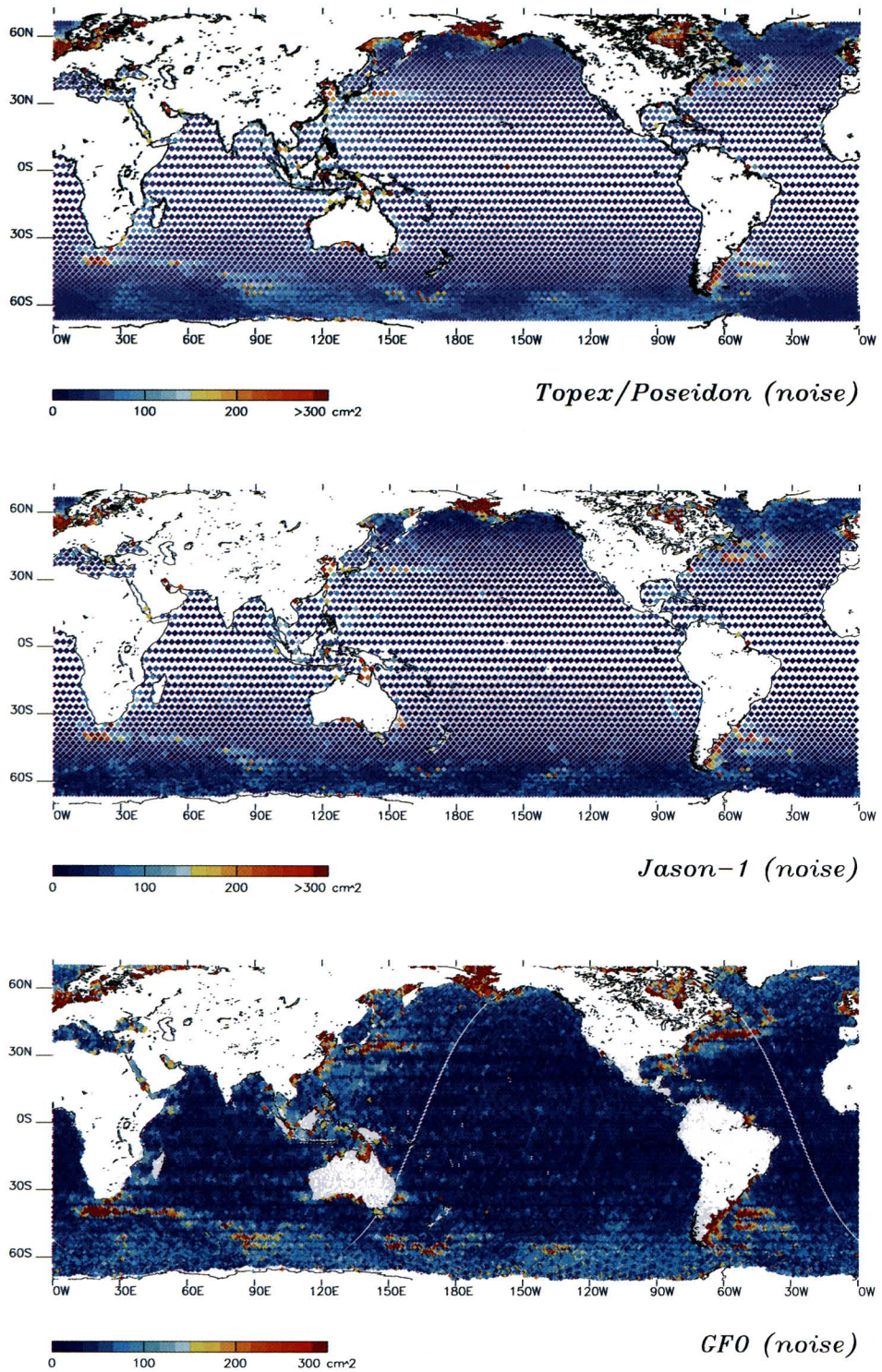

FIGURE 2 The variance of the noise, *var* $\langle \varepsilon \rangle$, as computed at each of the crossover points is plotted for each of the four altimeter missions. *(Continued)*

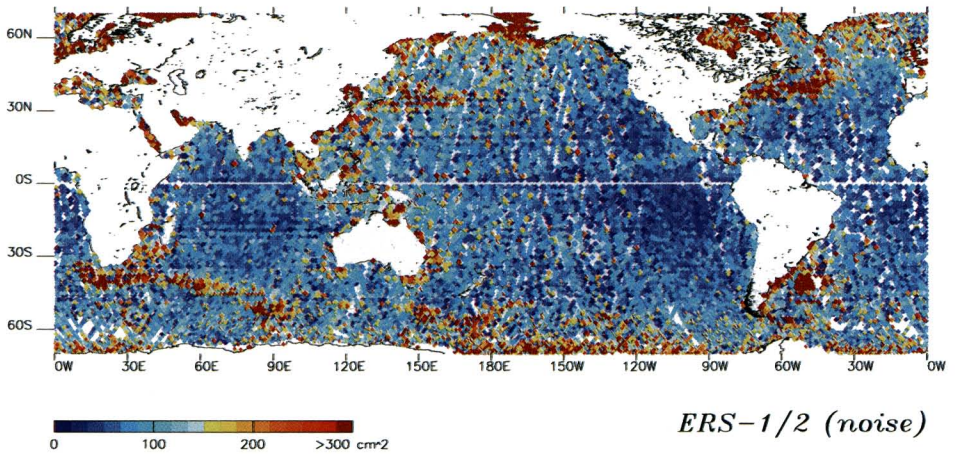

FIGURE 2 (Continued)

Overall, all four altimeter data set signal-to-noise ratios contain similar regional variations. The higher levels of noise associated with ERS-1/2 and GFO, and the latitudinal banding, however, make discerning these features much more difficult. The areas containing the most favorable signal-to-noise ratios are associated with baroclinic shear and known high eddy activity: the Kuroshio, Gulf Stream, Antarctic Circumpolar, and the Aghulus currents. Likewise, the areas with ratios well below unity include the high latitude regions and areas associated with lower overall ocean variability, such as the midlatitude regions west of South America and Africa. Shelf regions and semienclosed seas contain higher noise due to land contamination and domination by high frequency wind forced variability as well as errors in the tide solutions. Thus low signal-to-noise values are generally the result in these regions.

Within Jason-1 and T/P results in the North Pacific and Gulf of Mexico (Figures 4 and 5), similar values are obtained for the signal to noise ratio. In the North Pacific, Jason-1 produces many higher ratios than T/P, especially in the higher latitudes, but the results are much less consistent across the major current regions. Thus, it is easier to identify the contours surrounding these high variability systems and likewise the regions of low variability. In the Western Pacific semienclosed seas only a small percentage of the data points have ratios exceeding or approaching unity. The few higher ratio values in the semienclosed seas tend to be off the shelf, further from land, and in the deepest parts of the basin. Finally, quiescent regions with only small signals to measure, such as the Japan/East Sea, have very low ratios at almost all data points.

In the Gulf of Mexico (Figure 5), Jason-1 and T/P contain very similar results. Note that there are two more data points plotted for T/P than for Jason-1. This indicates that there are not enough good Jason-1 values at these points to compute a ratio. T/P benefits from the longer data time span in these cases. Note also that both these points are heavily corrupted by land—Mississippi River Delta and Caribbean Islands—and consequently, contain very low ratios for T/P. In all cases T/P produces equal or higher ratios than Jason-1. In the open basin all ratios are above unity except for one directly north of the Yucatan peninsula.

Navy Layered Ocean Model

A second approach to the calculation of the signal-to-noise ratio is performed using the results of the Navy Layered Ocean Model (NLOM) (Smedstad et al. 2002) for the signal

values. The NLOM is a 1/16 degree, eddy resolving, nearly global model running operationally at the Naval Oceanographic Office (NAVOCEANO) for real time prediction and monitoring of ocean features. It is a fully assimilative model, able to utilize all available altimetry data along track on a daily basis. For this study, the results of an 8-year run of the model (1993–2000) are used. The model uses all available T/P, ERS-1/2, and GFO data from this period. Note that no Jason-1 data is assimilated, as it is not active during this period. In calculating a signal to noise ratio, the SSHA variance is computed from the results of the model run. Only results from T/P are presented with the NLOM results. Similar results are obtained with the other altimeter data sets. The model results are interpolated in space to the T/P crossover points and SSHA variances computed. Note that the model does not contain shallow water areas (depths less than 200 m).

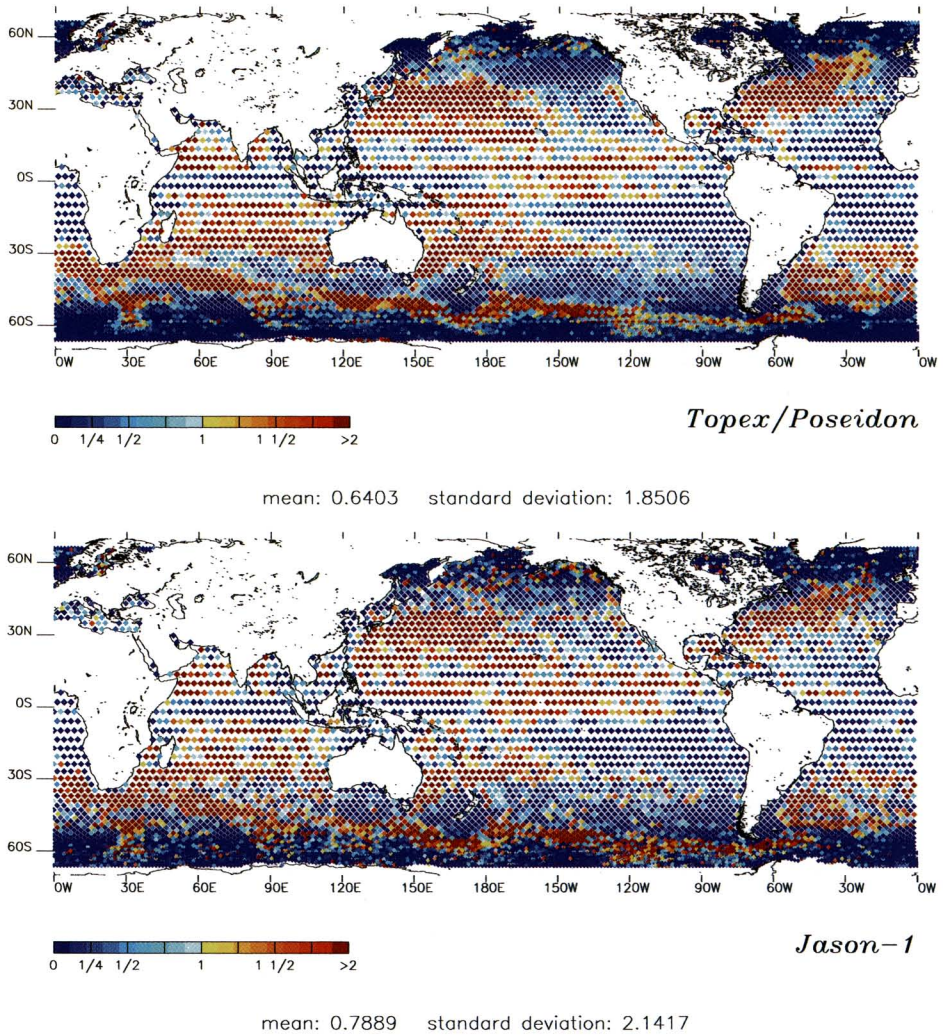

FIGURE 3 The signal-to-noise ration as computed at each of the crossover points is plotted for each of the altimeter missions: Topex/Poseidon (top), Jason-1 (bottom), full GFO (top next page), GFO restricted to crossover differences of less than five days (middle next page), full ERS-1/2 (bottom next page), ERS-1/2 restricted to crossover differences of less than five days (page after next). *(Continued)*

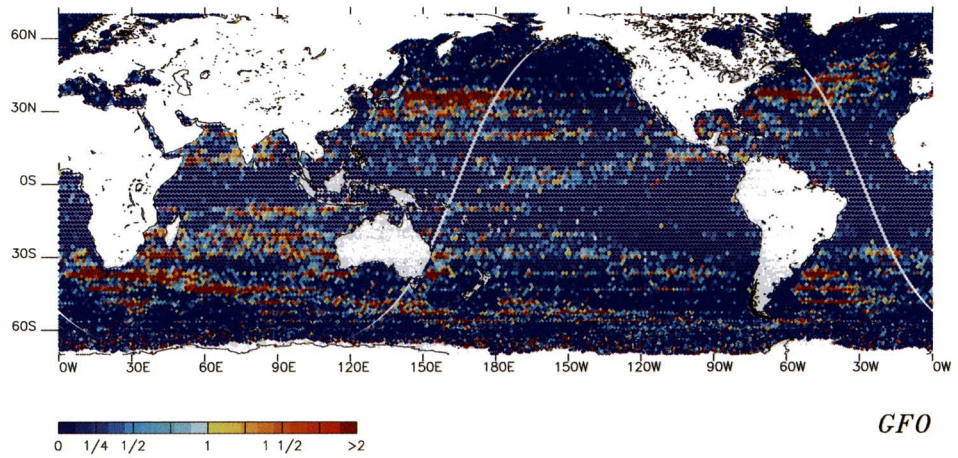

mean: 0.2441 standard deviation: 1.3949

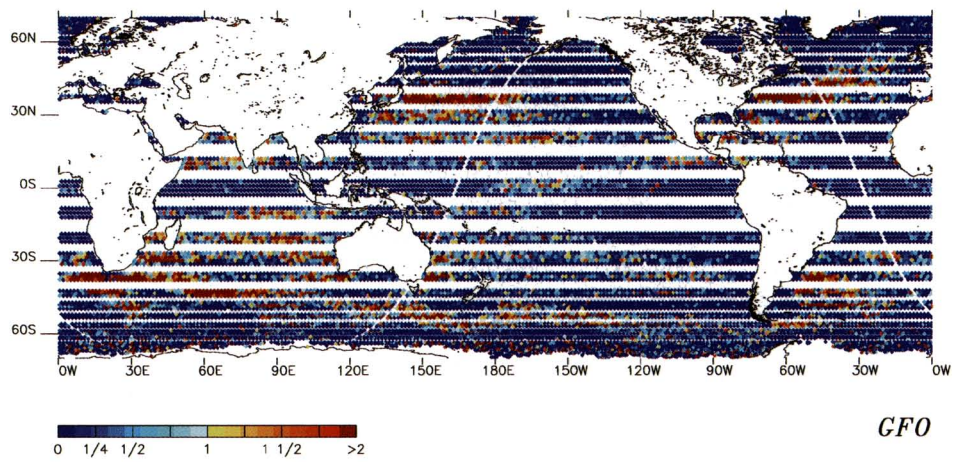

mean: 0.4340 standard deviation: 1.6465

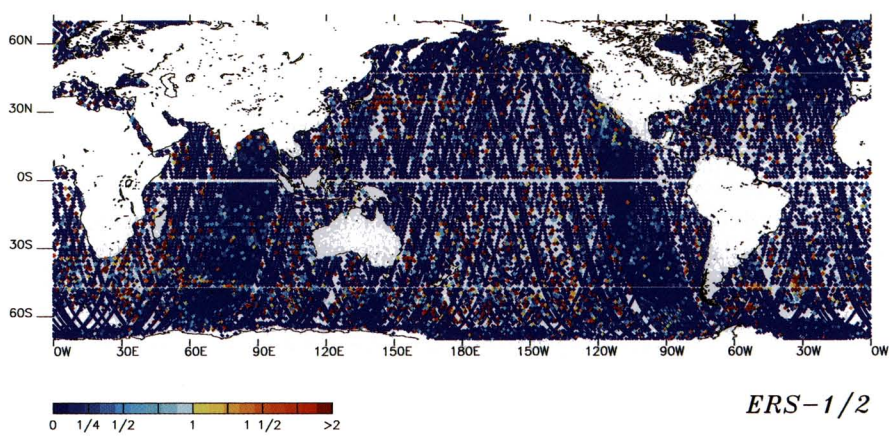

mean: −0.0574 standard deviation: 1.4684

FIGURE 3 *(Continued)*

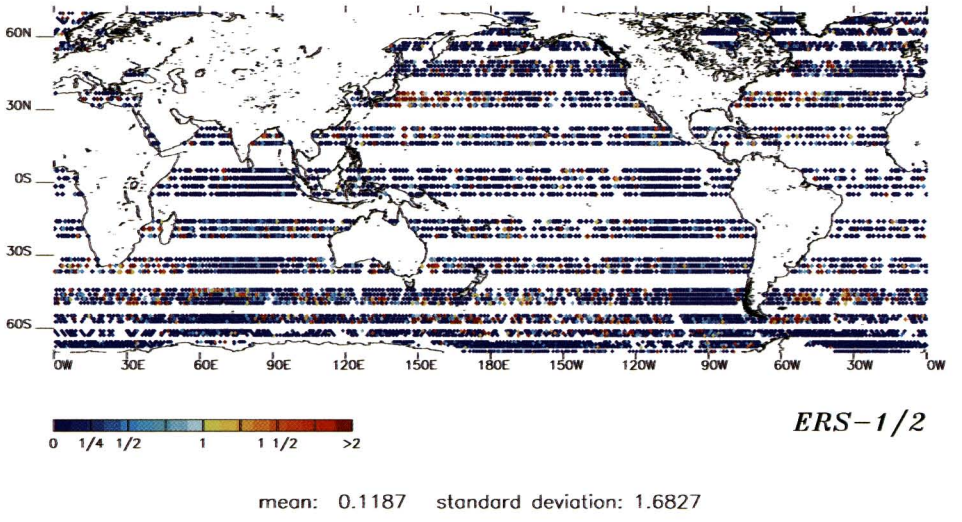

FIGURE 3 (Continued)

Figure 6 presents two additional views of the signal to noise ratio. The first uses the signal (SSH RMS variability) computed from the NLOM model output while using the noise from the T/P observations. The ratio of NLOM ocean signal to the T/P noise is presented only at T/P crossover points. The second view uses the signal and noise based on the NLOM output, where NLOM noise is computed from SSH changes between snapshots separated by five days. The NLOM results provide insight into the global sea surface height variability while employing knowledge from all available altimeters. Adding observations reduces the posteriori error covariance in an optimal interpolation. Thus, adding additional altimeter observations should reduce error levels of the NLOM height analyses. The results from the first study using NLOM produce a significantly higher global percentage of ratio values above unity, 43% as compared to 22% and 25% for T/P and Jason-1, respectively. One explanation is that the model removes the noise within the altimeter data that is uncorrelated between observations. A further explanation is related to the discussion above of how sea surface signal could be captured in the noise variance calculation. If this is the case, the ratio values calculated for the altimetry alone would be more adversely affected than that for the NLOM calculation. This is a direct result of the algebraic removal of the noise variance from the total variance to produce the sea surface height variance.

The second NLOM analysis using only the data from NLOM to compute the signal to noise calculation was constructed at each model grid point. The signal is defined as the RMS SSH variability at each point. The noise is defined as the SSH change model fields separated by five days. These values are linearly interpolated to the T/P crossover points to permit similar display in the plots and comparisons without introducing a regional sampling bias (Figure 6). Note that these ratios give an indication of the temporal sea surface height changes of five days or less but do not provide any information about altimeter measurement noise. The value of this calculation in this study is found in comparing it to the plot of signal to noise ratio for T/P (Figure 3). It provides further evidence of regions where the measurable sea signal, independent of altimeter measurement error, is low relative to the temporal part of the noise component of the ratio. This is mostly seen in the higher latitudes and known quiescent regions.

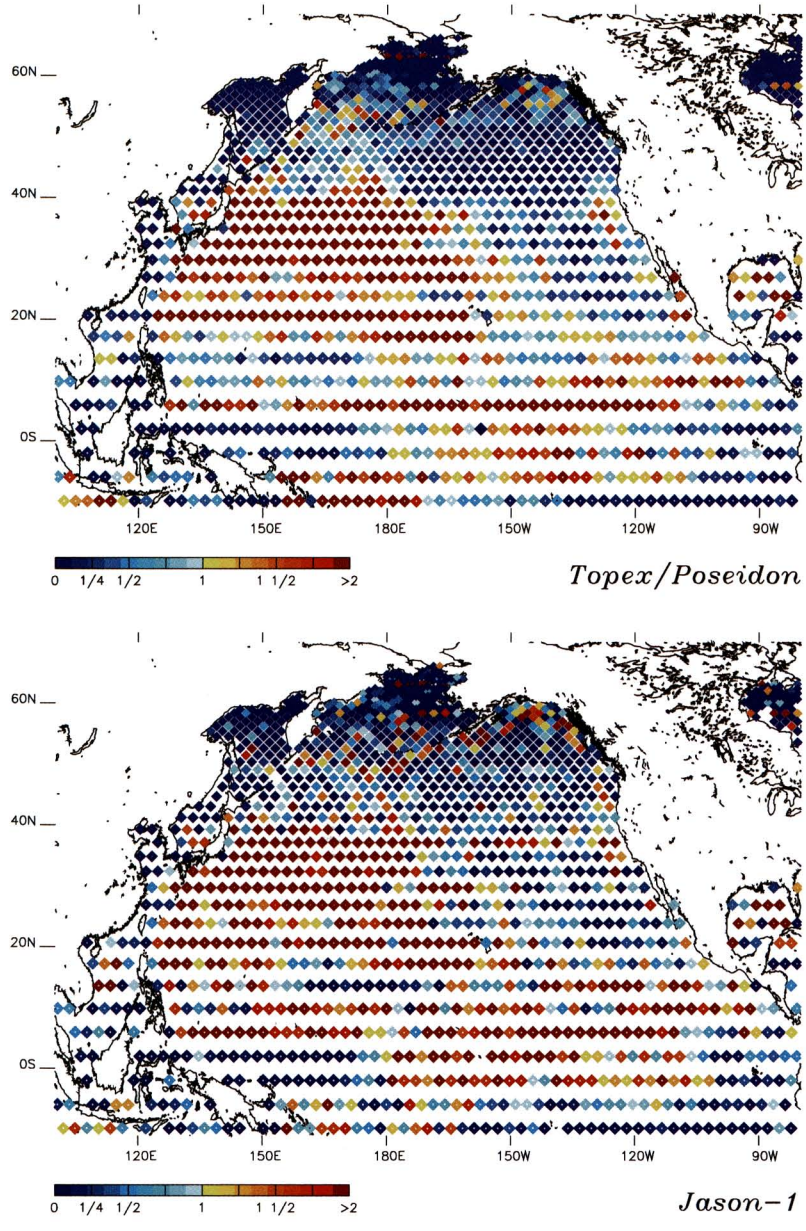

FIGURE 4 The signal-to-noise ratio is plotted for Topex/Poseidon (upper) and Jason-1 (lower) in the North Pacific.

Discussion

One basic assumption made in this study is that the ocean varies on time scales much greater than the crossover difference time (five days here) Breakdown in this assumption directly affects the calculation of the noise variance. Thus the noise defined here contains ocean processes that are not well resolved in time. The result is that the noise variance for a point actually contains some of the sea surface height variability signal. Regions experiencing high frequency variations in sea surface height are the most obvious candidates to be heavily affected by this. These are generally the shallower regions and the semienclosed

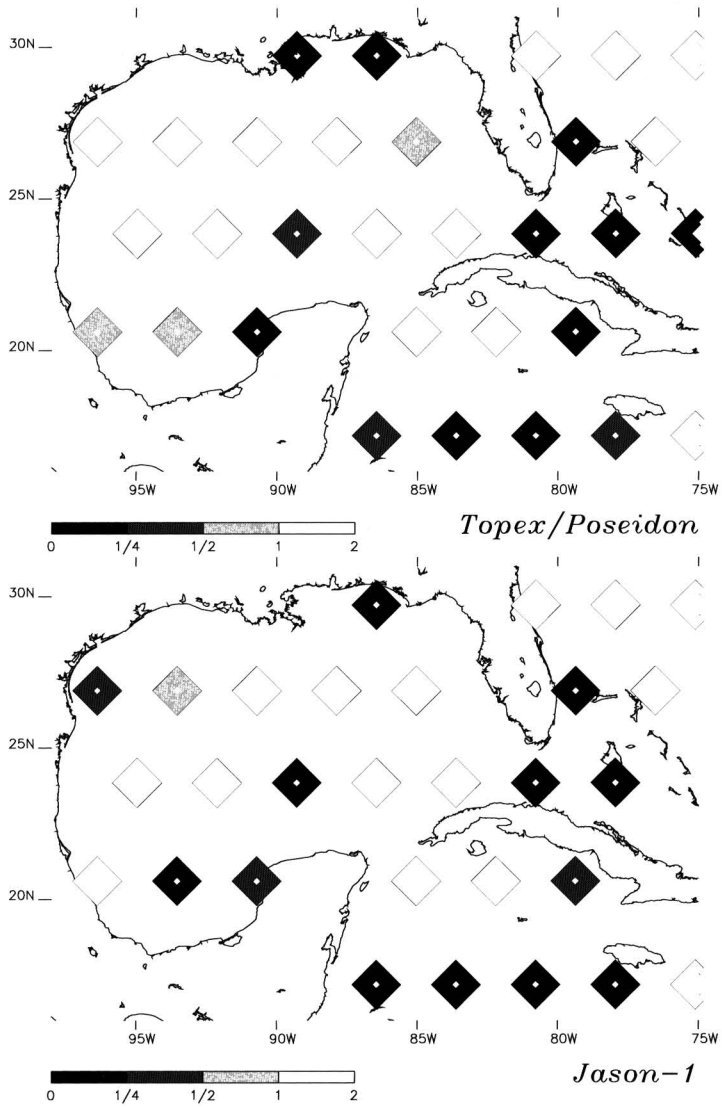

FIGURE 5 The signal-to-noise ratio is plotted for Topex/Poseidon (upper) and Jason-1 (lower) in the Gulf of Mexico.

seas. These regions are also the ones most prone to inaccuracies in ocean tide modeling and high frequency wind and pressure driven variability.

One particularly interesting observation is the signal to noise response in the western boundary currents. The signal is quite high in these fast flowing regions. As demonstrated in Figure 2, however, the noise is also quite high resulting from the mesoscale variability on the time scales of less than five days. Yet strong signal to noise values persist, generally greater than one and often much higher, in these regions. Traditionally, these regions have been some of the more difficult areas to model, and thus increased assimilation of data would be of great benefit. The numbers presented here show the value of the altimetry data to these regions.

Initially it is rather disappointing that a significant fraction of the global ocean has altimeter signal lower than the noise. If one considers, however, that one of the greatest strengths of altimetry is in measurement of meso and large scale features and also features that persist long enough to be measured by more than one pass of the altimeter, these values are not disheartening. The results examined so far are signal-to-noise estimates at single points. A single eddy would be observed by several points during one pass and subsequent passes over the eddy would add additional observations. Estimating that the RMS error in measuring a feature decreases with the square root of the number of points used in measuring it, ratio values of 0.5 and 0.25 would reach unity when a feature could be sampled by at

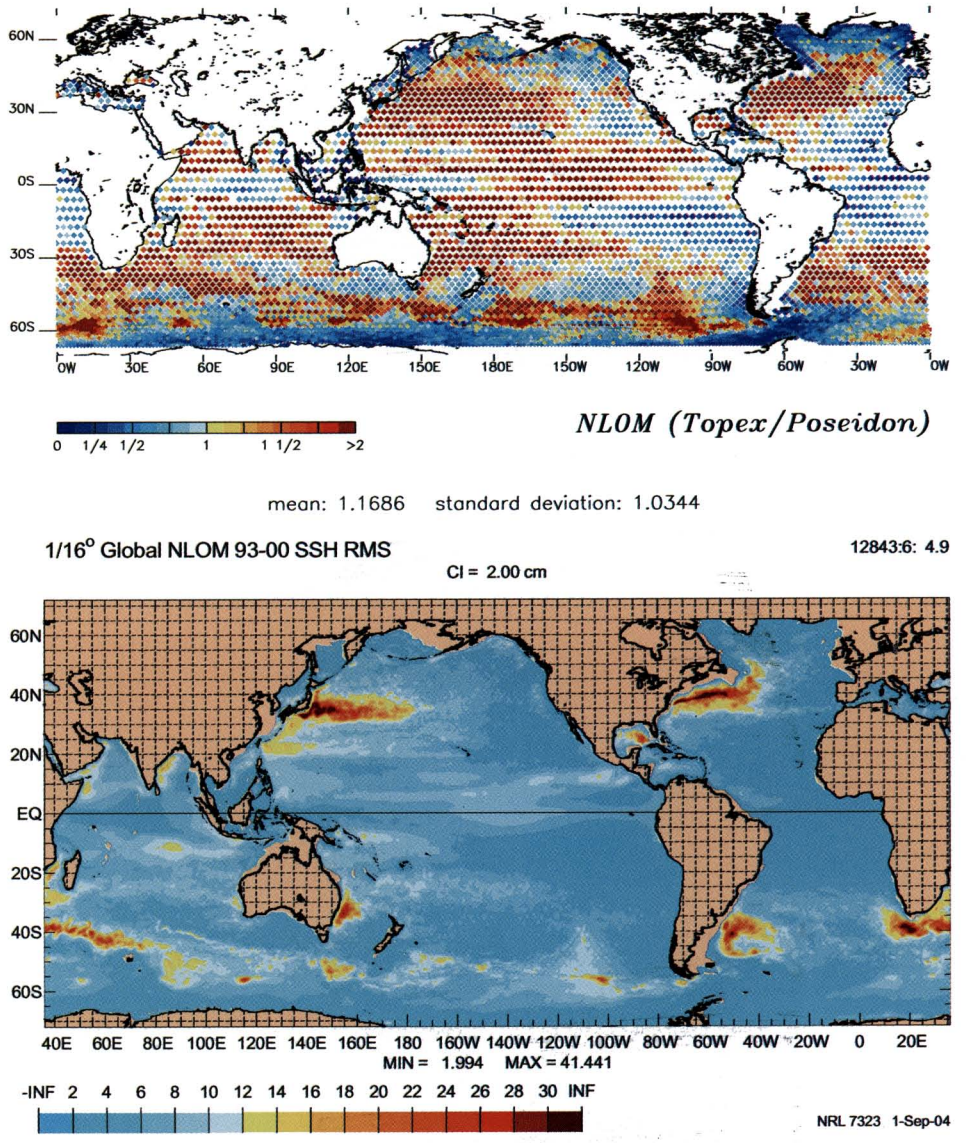

FIGURE 6 The NLOM model SSH RMS variability (bottom) provides the total signal according to the assimilating model. The ratio of NLOM signal to T/P noise is presented at the T/P crossover points (top). The signal-to-noise ratio based only on NLOM model output is interpolated to T/P crossover points (next page). *(Continued)*

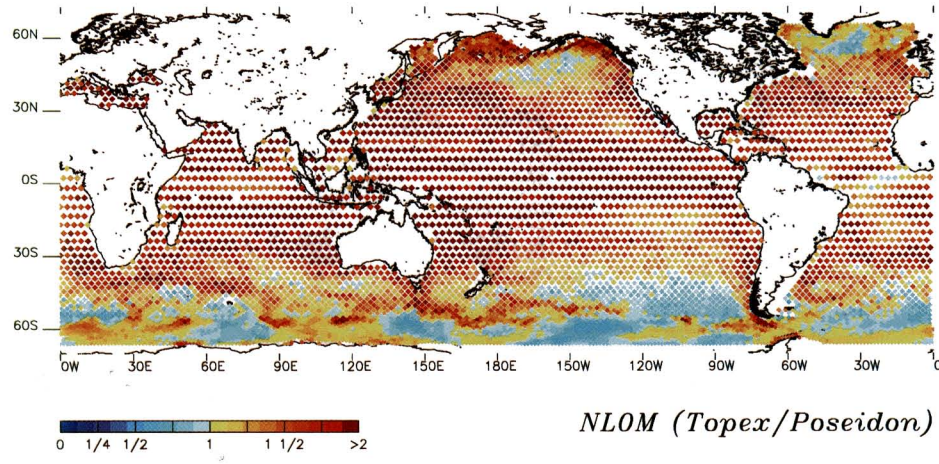

FIGURE 6 (Continued)

least four or 16 points, respectively. Only the smallest and most short lived features would not meet this criteria. This is especially promising when considering how altimetry data is assimilated into numerical ocean models used for monitoring or prediction of ocean features. A reexamination of Figures 3 through 5 shows that a large percentage of the data would meet the criteria of signal to noise ratio greater than 0.25. T/P and Jason-1 contain values greater than 0.25 for the majority of world oceans. Figure 7 clearly demonstrates how significant this is for Jason-1 globally. The results shown in the Gulf of Mexico (Figure 5) are also shown to be very promising. With the exception of the one point, all ratios in the main basin for T/P and Jason-1 provide positive signal to noise information in this light.

As mentioned above, T/P and Jason-1 demonstrate very similar signal to noise ratios, with Jason-1 slightly outperforming T/P on a global basis. Jason-1, however, appears to benefit from numerous higher values in the higher latitudes. To further investigate this, the global average signal to noise is examined within restricted latitude bands (Table 1). Each

TABLE 1 The Signal to Noise Ratios for Topex/Poseidon and Jason-1, as Presented in Figure 3, Tabulated by Numerical Range and Presented Within Decreasing Latitudinal Bounds (The Percentage of the Total Points for That Altimeter Within the Bounds is Given in Parentheses. The Mean and Standard Deviation Are Also Given.)

	<0.25	0.25–0.5	0.5–1.0	>1.0	Mean/Std.Dev.
T/P (All)	10590 (56)	1748 (9)	2203 (12)	4207 (22)	0.64/1.85
Jason (All)	9571 (53)	1696 (9)	2208 (12)	4618 (25)	0.79/2.14
T/P ±60°	4183 (37)	1265 (11)	1852 (16)	3942 (35)	1.10/1.99
Jason ±60°	4578 (45)	1070 (10)	1572 (15)	3956 (39)	1.20/2.54
T/P ±55°	2812 (32)	1003 (11)	1462 (17)	3427 (39)	1.27/2.14
Jason ±55°	3284 (38)	816 (9)	1291 (15)	3277 (38)	1.33/2.73
T/P ±50°	2000 (29)	820 (12)	1208 (17)	2936 (42)	1.40/2.28
Jason ±50°	2388 (34)	678 (10)	1078 (16)	2786 (40)	1.45/2.86
T/P ±45°	1586 (27)	687 (12)	1043 (18)	2588 (44)	1.43/2.31
Jason ±45°	1927 (33)	588 (10)	924 (16)	2433 (41)	1.50/2.92

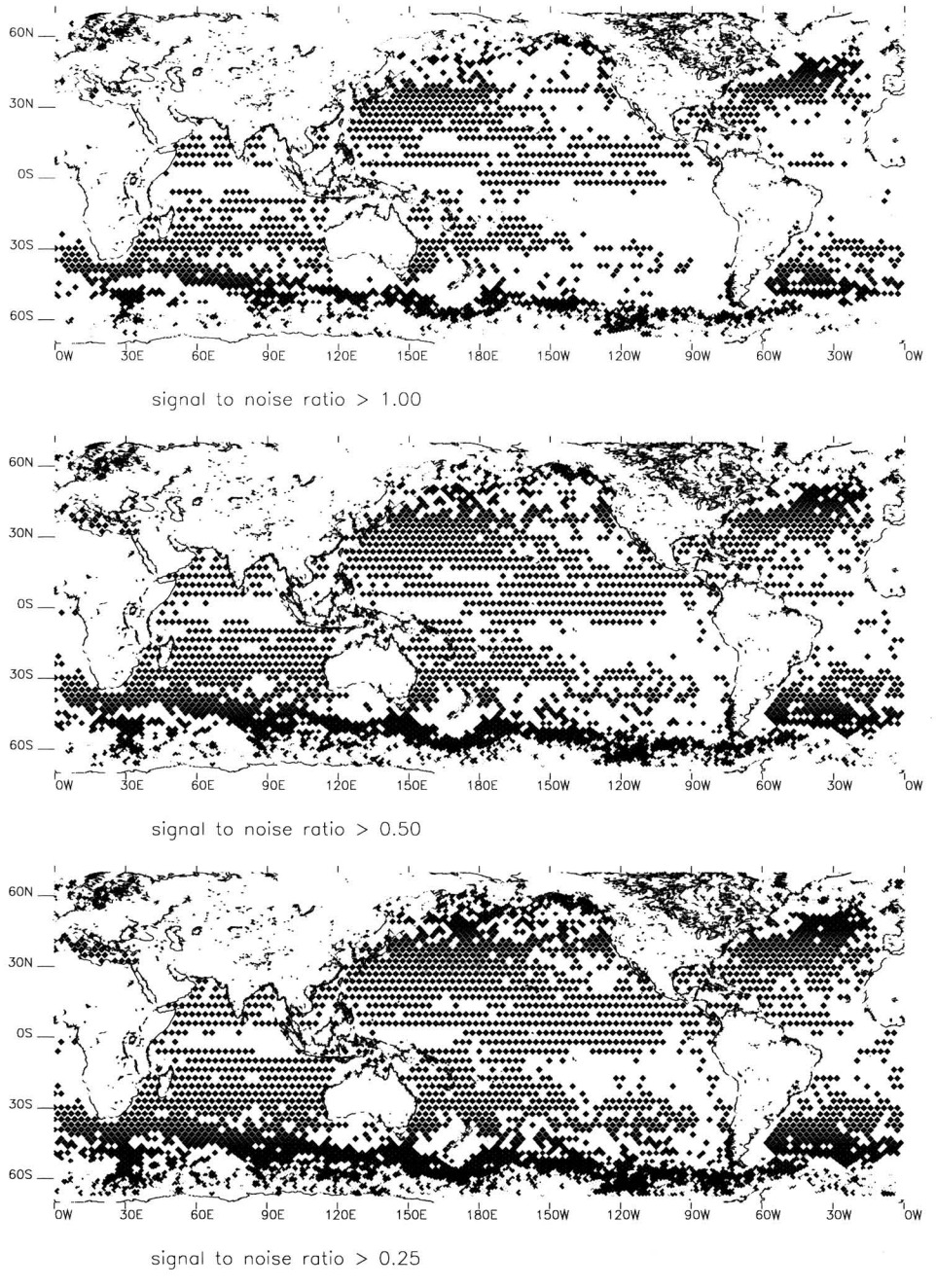

FIGURE 7 The signal-to-noise ratio is presented for Jason-1. In the upper plot all values greater than 1 are plotted. In the middle plot all values greater than 0.5 are plotted. In the lower plot all values greater than 0.25 are plotted.

column represents the number of ratio values that fall within a certain range. These ranges correspond to the discussion above in which a feature would be accurately resolved by more than 16 points, four points, or one point, respectively. In addition, the percentage of the total number of crossover points is given. The mean and standard deviation are given for reference. As expected, both altimeter data sets improve as the values are included from

only lower latitudes. The values for T/P, however, improve at a greater rate and begin to outperform Jason-1 when the values are constrained by ±55°. Within ±45°, 74% of the world's ocean features can be accurately resolved when sampled by at least 16 T/P points, compared to only 67% for Jason-1. And yet, the Jason-1 mean is still higher. This fact remains true for all the latitudinally bounded regions presented. This would tend to indicate that the values greater than one for Jason-1 are higher than those for T/P. This is further indicated by the higher standard deviation values.

Conclusions

As expected the high variability large current regions contain the most consistently high signal-to-noise ratios. Much can be discerned through closer inspection of the semienclosed seas and other specific areas. This is most valuable as the topic of high frequency sea level response, so common in these areas, is further studied. Improvements in the modeling of high frequency changes in SSH in response to winds and surface pressure are currently being studied and implemented into the processing of altimetry data. These and other higher frequency signals currently alias into the measurements and can appear as noise. One possible outcome of this study is the development of a regional weighting matrix for the utilization or assimilation of altimetry data. Especially in models such as NLOM (Smedstad 2000) which assimilate altimetry data along track, this information will prove to be invaluable. In addition, the signal to noise ratio is also a good benchmark value for measuring improvements to altimetry data processing.

References

Blayo, E., J. Verron, and J. M. Molines. 1994. Assimilation of Topex/Poseidon altimeter data into a circulation model of the North Pacific. *J. of Geophys. Res.* 99(C12):24691–24705.

Blayo, E., T. Mailly, B. Barnier, P. Brasseur, C. LeProvost, J. M. Molines, and J. Verron. 1997. Complementarity of ERS 1 and Topex/Poseidon altimeter data in estimating the ocean circulation: Assimilation into a model of the North Atlantic. *J. of Geophys. Res.* 102(C8):18573–18584.

Chen, G., S. W. Bi, and R. Ezraty. 2004. Global structure of extreme wind and wave climate derived from TOPEX Altimeter Data. *Int. J. of Remote Sensing* 25:1005–1018.

Fox, A. D., K. Haines, B. A. de Cuevas, and D. J. Webb. 2000a. Altimeter assimilation in the OCCAM Global Ocean Model Part I: A twin experiment. *J. of Marine Sys.* 26:303–322.

Fox, A. D., K. Haines, B. A. de Cuevas, and D. J. Webb. 2000b. Altimeter assimilation in the OCCAM Global Ocean Model Part II: Topex/Poseidon and ERS-1 assimilation. *J. of Marine Sys.* 26:323–347.

Hallock, Z. R., J. L. Mitchell, and J. D. Thompson. 1989. Sea surface topographic variability near the New England Seamounts: An intercomparison among in situ observations, numerical simulations, and Geosat altimetry from the Regional Energetics Experiment. *J. Geophys. Res.* 94:8021–8028.

Jacobs, G. A., C. N. Barron, and R. C. Rhodes. 2001. Mesoscale characteristics. *J. Geophys. Res.* 106:19581–19595.

Robinson, A. R., P. F. J. Lermusiaux, and N. Q. Sloan III. 1998. Data assimilation. pp. 541–593. *In The Sea, Vol. 10*, K. H. Brink and A. R. Robinson, eds. John Wiley and Sons.

Sandwell, D. T., and W. H. F. Smith. 1997. Marine gravity anomaly from Geosat and ERS-1 altimetry. *J. of Geophys. Res.* 102(B5):10039–10054.

Schouten, M. W., W. P. M. de Ruiter, and P. J. van Leeuwen. 2000. Translation, decay and splitting of Agulhas rings in the southeastern Atlantic Ocean. *J. of Geophys. Res.* 105(C9):21913–21925.

Schrama, E. J. O., and R. D. Ray. 1994. A preliminary tidal analysis of TOPEX/Poseidon altimetry. *J. of Geophys. Res.* 99(C12):24799–24808.

Segschneider, J., D. L. T. Anderson, and T. N. Stockdale. Toward the use of altimetry for opperational seasonal forecasting. *J. of Climate* 13:3115–3138.

Smedstad, O. M., H. E. Hurlburt, E. J. Metzger, R. C. Rhodes, J. F. Shriver, A. J. Wallcraft, and A. B. Kara. 2002. An operational eddy resolving 1/16° Global Ocean Nowcast/Forecast System. *J. of Marine Systems* 40–41:341–361.

Teague W. J., M. J. Carron, and P. J. Hogan. 1990. A comparison between the generalized digital environmental model and Levitus climatologies. *J. of Geophys. Res.* 95(C5):7167–7183.

Zanifé, O. Z., P. Vincent, L. Amarouche, J. P. Dumont, P. Thibaut, and S. Labroue. 2003. Comparison of the Ku-Band range noise level and the relative sea-state bias of the Jason-1, TOPEX, and Poseidon-1 radar altimeters. *Mar. Geod.* 26:201–238.